A study of frequency and size distribution dependence of extinction for astronomical silicate and graphite grains

Ashim K. Roy[1]*Subodh K. Sharma[2] and Ranjan Gupta[3]

[1]Indian Statistical Institute, 203, BT Road, Kolkata 700108, India
[2] S N Bose National Centre for Basic Sciences, Kolkata 700098, India
[3] Inter University Centre for Astronomy and Astrophysics, Pune 411007, India

April 6, 2009

*E-mail:ashim@isical.ac.in (AKR); sharma@ose.res.in (SKS); rag@iucaa.ernet.in (RG)

Abstract

It is generally agreed that interstellar dust grains consist of two main components, namely, silicates and graphites. Some models, like MRN model, assume these grains to be homogeneous spheres following a power law size distribution. This paper presents, in the framework of Mie theory, a parametrization of extinction spectrum curves of the silicates and the graphites separately in terms of frequency and the minimum and maximum of sizes in the distribution. Analytic expressions in ultraviolet and far-ultraviolet are presented for both types of grains.The values of maximum and minimum sizes for which these equations are valid have been identified. These equations can be useful in a number of situations involving silicate and graphite grains.

1 Introduction

In a recent publication we analyzed extinction spectrum of a collection of homogeneous spherical particles of a unknown size distribution [1] (hereafter referred as RS-I). It was shown that an extinction spectrum, in general, has some easily identifiable characteristic regions where the extinction-frequency relationship can be approximated by simple empirical formulae involving first four moments of the particle size distribution. The analysis clearly exhibited the manner in which essential features of the particle size distribution gets coded into its extinction spectrum (more generally known as the Interstellar Extinction Curve in the astrophysical situation). It was demonstrated that the moments could indeed be obtained from its extinction spectrum and that with the knowledge of these moments it was possible to reconstruct the size distribution function.

The analysis in RS-I however, assumed that all particles were of same material for which the refractive index did not vary with frequency. The question arises what happens when a collection of particles has more than one material component with their refractive indices varying with wavelength. We address ourselves to these questions in this paper. In other words, the purpose of this work is to examine the possibility of extending the ideas developed in RS-I to a multi-component system where refractive index of the individual components varies with wavelength of incident electromagnetic radiation.

One suitable model where these extensions of RS-I can be studied is a modified version of interstellar dust model due to Mathis, Rumpl and Nordsieck (MRN) [2]. The MRN model assumes that interstellar dust consists of individual grains of homogeneous spheres of silicates and graphites having very definite power-law size distributions. For graphite grains, there is a "$\frac{1}{3} - \frac{2}{3}$" approximation [3]. This modification essentially converts two component MRN model to a three component MRN model. Investigations in this work show that the frequency-size relationship can still be obtained even when the refractive index of the

grains is varying with wavelength. But, because of rapid variation of refractive index with frequency, now one needs to divide the spectrum in suitable intervals and obtain separate relations for each sub-interval. This paper presents these relationships in ultraviolet and far-ultraviolet frequency domains for silicate and graphite grains individually. Thus, we not only demonstrate, the successful extension of ideas in RS-I to materials whose refractive index varies with wavelength, but in the process we also present relationships which can be used for testing various models of interstellar dust.

This paper is organized as follows. Section 2 describes the dust model considered here. Section 3 gives the functional form of extinction in terms of size distribution parameters as well as the frequency for both graphite and silicate grains. Subsequently, numerical results of extinction obtained from these formulae are compared with exact Mie theory computations in section 3. The possible use of such formulae for individual components to multi-component system has been demonstrated in section 4. Finally, we conclude by summarizing and discussing the results of this paper in section 5.

2 The Dust Model

A classic model of interstellar dust was proposed more than 30 years ago by Mathis, Rumpl and Nordsieck (MRN) (1977). Since then, the basic model is being used even today albeit with some modifications. It has not been fully superseded by later studies. The MRN model uses two separate populations of bare silicate and graphite grains with a power-law distribution of sizes of the form:

$$f(a) \propto a^{-3.5} \qquad a_0 \leq a \leq a_m, \tag{1}$$

where a denotes the radius of the spherical grain varying within the limits a_0 (minimum radius) and a_m (maximum radius). The size range for graphite and silicate grains is:

$$Graphite\ grains: \qquad a_0 \sim 0.005\mu m \qquad a_m \sim 0.25\mu m, \tag{2}$$

$$\textit{Silicate grains}: \quad a_0 \sim 0.005\mu m \quad a_m \sim 0.25\mu m. \tag{3}$$

Further, the graphite material is supposed to be present in two distinct structural varieties within the specified range of a_0 and a_m. This plausibility lies in the fact that graphite is highly anisotropic material. The refractive index of graphite, therefore, depends on the orientation of electric field relative to the structural symmetry. Owing to difficulties in calculations of exact scattering quantities due to anisotropy, workers have taken resort to an approximation known as "$\frac{1}{3} - \frac{2}{3}$" approximation [3]. In this approximation graphite grains are represented as mixture of isotropic spheres, $\frac{1}{3}$ of which have refractive index $m = m_{\parallel}$ (referred as graphite parallel) and $\frac{2}{3}$ have the refractive index $m = m_{\perp}$ (referred as graphite perpendicular). This modification effectively makes MRN model a three component model.

3 Extinction as a function of frequency and size distribution parameters

Exact extinction coefficient, K_{ext}, was obtained using the formula,

$$K_{ext}(\lambda) = \pi N \int_{a_0}^{a_m} Q_{ext}(x) a^2 f(a)\ da, \tag{4}$$

where $Q_{ext}(x)$ is the extinction efficiency of an individual scatterer of size parameter x and $x = 2\pi a/\lambda$ with λ as the wavelength of the radiation. The exact extinction efficiency Q_{ext} for a spherical homogeneous scatterer can be computed using Mie formulas. The necessary refractive index particulars for various components (at various wavelengths) were taken from the tables provided by Draine [4] on his website. The number of particles per unit volume, N has been arbitrarily fixed at $N = 4.4 \times 10^8$. in these calculations. This being a multiplicative constant, its admitted value does not make any effective difference in the functional form of K_{ext} we wish to determine.

In case of size distributions of spherical particles having constant refractive index (wavelength independent) it was shown in RS1 that in the $K_{ext} - \nu$ graph, in general, we can

identify frequency intervals where K_{ext} has distinctly linear or parabolic or asymptotic behaviour having corresponding functional forms of K_{ext}:

$$K_{ext}^{(L)} \sim l_1(m)\bar{a^3}\nu + l_2(m)\bar{a^2},$$

$$K_{ext}^{(P)} \sim p_1(m)\bar{a^4}\nu^2 + p_2(m)\bar{a^3}\nu + p_3(m)\bar{a^2},$$

etc., where, l_1, l_2, p_1, p_2, p_3 are coefficients which have arbitrary dependence on refractive index m. $\bar{a^2}, \bar{a^3}$ and $\bar{a^4}$ are the 2nd, 3rd and 4th raw moments of the size distribution $f(a)$.

In the present situation, where m varies with ν, the coefficients l_1, l_2, p_1, p_2, p_3 will also show variation with ν and hence the distinctly simple linear and parabolic forms of K_{ext} will not be observed within a meaningful frequency interval. Hence, our approach has been to study the $K_{ext} - \nu$ graph for each material component separately for various ranges of a, which means varying a_0, a_m. In case of the power-law size distribution, $f(a) = ca^{-3.5}$, we have relations:

$$\begin{aligned}
c &= \frac{5}{2}a_0^{5/2}\Big(1 - \frac{1}{n^5}\Big)^{-1}, \\
\bar{a} &= \frac{5}{3}a_0\Big(1 - \frac{1}{n^3}\Big)\Big(1 - \frac{1}{n^5}\Big)^{-1}, \\
\bar{a^2} &= 5a_0^2\Big(1 - \frac{1}{n}\Big)\Big(1 - \frac{1}{n^5}\Big)^{-1}, \\
\bar{a^3} &= 5a_0^3\Big(n - 1\Big)\Big(1 - \frac{1}{n^5}\Big)^{-1}, \\
\bar{a^4} &= \frac{5}{3}a_0^4\Big(n^3 - 1\Big)\Big(1 - \frac{1}{n^5}\Big)^{-1},
\end{aligned}$$

where $n = (a_m/a_0)^{1/2}$. Consequently, with a functional form $K_{ext}(a_0, a_m, \nu)$, our investigations reveal that the extinction in the UV and FUV regions for the materials considered have the following general form:

$$K_{ext} = CNa_0^{5/2}\Big[\phi(a_0, \nu) + \psi(a_m, \nu)\Big]. \tag{5}$$

The functions ϕ and ψ have forms which change in various frequency sub-intervals. For each component of graphite (parallel and perpendicular), four formulae were needed to fit

extinction. For silicate, three formulae were sufficient. Several values of a_m and a_0 were considered. Formulae presented here are valid in the size limits:

$$Graphite\ grains: \quad 0.002\mu m \leq a_0 \leq 0.005\mu m; \quad 0.15\mu m \leq a_m \leq 0.25\mu m, \tag{6}$$

$$Silicate\ grains: \quad 0.004\mu m \leq a_0 \leq 0.006\mu m; \quad 0.2\mu m \leq a_m \leq 0.4\mu m. \tag{7}$$

Observations of the spectra suggested that the functions $\phi(a_0, \nu)$ and $\Psi(a_m, \nu)$ can have the simple forms:

$$\phi(a_0, \nu) = b_0(\nu) + a_0^{1/2} b_1(\nu) + a_0 b_2(\nu)$$

$$\Psi(a_m, \nu) = \frac{c_0(\nu)}{a_m^{1/2}} + \frac{c_1(\nu)}{a_m} + \frac{c_2(\nu)}{a_m^2} + \frac{c_3(\nu)}{a_m^3} + ...,$$

where a_0, a_m are taken in units of $10^{-5}cm$, ν in units of $10^5 cm^{-1}$. The number of significant terms contributing to extinction in ϕ and Ψ depend on the material as well as the frequency interval considered. The forms of $\phi(a_0, \nu)$ and $\Psi(a_m, \nu)$ have been constructed by careful analysis of the regional (frequency sub intervals) behaviour of the extinction for each of the materials considered. In the process of developing analytic formulae, care has been taken to have a good compromise between accuracy and calculational simplicity so that our analysis could be applied expediently for purposeful dust modelling within the power law framework considered here.

Following relationships have been obtained:

3.1 Homogeneous graphite grains with refractive index $m = m_\perp$

1. For $1000 \leq \lambda \leq 1460$**Å (FUV region I)**:

$$K = C a_0^{5/2} \Big[\nu^2 \Big(0.259 + 20.3073(\nu - 0.8485)^4 \Big) - (\nu a_0)^{1/2} \Big(0.267\nu - 0.16048 +$$

$$71.15(\nu - 0.8428)^4 \Big) - a_0 \nu^{5/2} \Big(0.0458\nu + 0.0164 +$$

$$14.8274(\nu - 0.8428)^2(\nu - 0.67905) \Big) - 0.0488 \Big(\frac{1}{a_m^{1/2}} + \frac{0.1551}{a_m} \Big) \Big] \tag{8}$$

2. For $1460 \leq \lambda \leq 1900$**Å (FUV region II)**:

$$K = Ca_0^{5/2}\Big[1.97754 - \frac{2.42703}{\nu} + \frac{0.79483}{\nu^2} - \frac{a_0^{1/2}}{\nu^2}\Big(0.2164 - 0.27812\nu + \frac{0.43347}{\nu^{1/4}}(1.0 - \frac{0.6856}{\nu})$$

$$(1.0 - \frac{0.5263}{\nu})\Big) - \frac{a_0}{2\nu^2}\Big((1.0 - \frac{0.606}{\nu})^2 + \frac{0.03173}{\nu}(1 - \frac{0.6262}{\nu}) - 46.52\nu(\nu - 0.6856)$$

$$(\nu - 0.5263)(\nu - 0.606)\Big) - 0.0488(\frac{1}{a_m^{1/2}} + \frac{0.1551}{a_m})(0.8667 + 24.1(\nu - 0.6112)^2)\Big]. \qquad (9)$$

3. For $1900 \leq \lambda \leq 2500$**Å (UV region I)**:

$$K = Ca_0^{5/2}\Big[\frac{1}{2.7 + 490(\nu - 0.4654)^2} + 100|\nu - 0.4654|^3 - \nu a_0^{1/2}\Big(\frac{1}{1.1058 + 6.5985|\nu - 0.4736|}$$

$$+11307(\nu{-}0.4673)^4{-}258.26\nu(\nu{-}0.4759)^2\Big){-}a_0\Big(\frac{0.0813}{1.0 + 6.9(1.0 - \frac{0.4566}{\nu}) + 76.187\nu|\nu - 0.4566|)}\Big)$$

$$-0.05511\Big(\frac{1}{a_m^{1/2}} + \frac{0.2398}{a_m}\Big)\Big(1.9503 - 1.712\nu + 0.583|\nu - 0.452|\Big)\Big]. \qquad (10)$$

4. For $2500 \leq \lambda \leq 4000$**Å (UV region II)**:

$$K = Ca_0^{5/2}\Big[\nu^{1/2}\Big(0.1161 + 0.60\nu - 1.9684\nu^{1/4}(0.4 - \nu)^{1/2}(\nu - 0.25)\Big) - a_0^{1/2}\nu^2\Big(0.461+$$

$$1.7567|\nu - 0.325| + 180.6(\nu - 0.325)^3\Big) - a_0\nu^3\Big(20664(\nu - 0.3244)^4+$$

$$\frac{1.3019\nu}{1.0 + 304.9(1.0 - \frac{0.3229}{\nu})^2}\Big) - 0.0507\Big(\frac{1}{a_m^{1/2}} + \frac{0.278}{a_m}\Big)\Big] \qquad (11)$$

3.2 Homogeneous graphite grains with refractive index $m = m_{\|}$

1. For $1000 \leq \lambda \leq 1120$**Å (FUV region I)**:

$$K = Ca_0^{5/2}\Big[\nu^{3/2}\Big(0.3473 - 6.284(1 - \nu)^2\Big) - a_0^{1/2}\nu^{3/2}\Big(2.3047\nu - 2.0047+$$

$$1.38(1 - \frac{0.901}{\nu})(\frac{1}{\nu} - 1)^{1/2}\Big) - a_0\Big(5.55(\frac{1}{\nu} - 1)^{1/2}(1 - \frac{0.901}{\nu})|1 - \frac{0.9524}{\nu}|^{1/2}+$$

$$\frac{0.2979}{\nu^{1/2}} - \frac{11.65}{\nu^{1/2}}(1 - \nu)^2\Big) - \Big(\frac{0.046}{a_m^{1/2}} + \frac{0.011}{a_m}\Big)\Big]. \qquad (12)$$

2. For $1120 \leq \lambda \leq 1500$**Å (FUV region II)**:

$$K = Ca_0^{5/2}\Big[0.06685 - 0.06056\nu + 0.277\nu^2 - a_0^{1/2}\Big(0.15482\nu - 0.07954\Big) -$$

$$a_0\Big(0.75484\nu - 0.495\Big) - 0.018\Big(\frac{2}{a_m^{1/2}} + \frac{1}{a_m}\Big)\Big] \tag{13}$$

3. For $1500 \leq \lambda \leq 2400$**Å (FUV region III)**:

$$K = Ca_0^{5/2}\Big[\frac{1}{\nu^{1/2}}\Big(0.0864 + \frac{0.79}{\nu}(\nu - 0.4675)^2 - 7.16(\nu - 0.49)^4\Big) - \frac{a_0^{1/2}}{\nu^{5/2}}\Big(0.0065 +$$

$$\frac{0.06575}{\nu}(\nu - 0.4922)^2 - 1.76(\nu - 0.5112)^4\Big) - a_0\Big(0.0054 + \frac{0.24|\nu - 0.5263|}{1.0 + 118(nu - 0.5405)^2}\Big)$$

$$-\frac{0.03913 + 0.07925|\nu - 0.5311|}{a_m^{1/2}} - \frac{0.008 - 0.2116(\nu - 0.5486)^2}{\nu a_m}\Big] \tag{14}$$

4. For $2400 \leq \lambda \leq 4000$**Å (UV)**:

$$K = Ca_0^{5/2}\Big[0.1495 - \frac{0.0847}{\nu}|\nu - 0.3675| - a_0^{1/2}\Big(\nu(0.1915 - 0.817|\nu - 0.3719|) -$$

$$33.0|\nu - 0.3675|(0.4167 - \nu)(\nu - 0.25)^2\Big) - a_0\frac{0.00356}{(1 + 15.017|\nu - 0.4031|)^2} -$$

$$\frac{0.26}{a_m^{1/2}}\nu(1.0 - 1.36\nu) - \frac{0.00436 + 0.0122\nu|\nu - 0.3542|}{a_m\nu}\Big] \tag{15}$$

3.3 Homogeneous silicate grains

1. For $1000 \leq \lambda \leq 1460$**Å (FUV region I)**:

$$K = Ca_0^{5/2}\Big[0.11668 - 0.02745\nu + 0.17\nu^2 - a_0^{1/2}\Big(0.3542\nu - 0.2110\Big) -$$

$$-a_0\Big(0.6677\nu - 0.3733\Big) + \Big(2a_m(1 - \nu)(\nu - 0.6856) - \frac{0.05}{a_m^{1/2}} - \frac{0.0062}{a_m}\Big)\Big] \tag{16}$$

2. For $1460 \leq \lambda \leq 2000$**Å (FUV region II)**:

$$K = Ca_0^{5/2}\Big[0.29168\nu - 0.02268 - a_0^{1/2}\Big(0.0634\nu - 0.01623\Big) -$$

$$a_0\Big(0.64634\nu - 0.3478\Big) - \Big(\frac{0.05}{a_m^{1/2}} + \frac{0.0062}{a_m}\Big)\Bigg] \tag{17}$$

3. For $2000 \leq \lambda \leq 4000$**Å (UV)**:

$$K = Ca_0^{5/2}\Bigg[-0.02833 + 0.197\nu + \frac{0.00669}{\nu} + 0.006567a_m\nu - \frac{0.0151}{a_m^2\nu} -$$

$$-\frac{0.016417}{a_m^3}\Big(\frac{1 - 4|1 - \frac{0.435}{\nu}|}{(1.0 + 10|1 - \frac{0.435}{\nu}|)^2}\Big)\Bigg] \tag{18}$$

In all the above formulae (8)-(18), $C = \pi N/10^8$; a_0, a_m are in units of $10^{-5}cm$; ν in units of $10^5 cm^{-1}$.

4 Numerical comparisons

Figure 1 shows a comparison of exact extinction curves with predictions of formula for graphite grains. The "$\frac{1}{3} - \frac{2}{3}$" approximation has been used in these comparisons. The three graphs presented in this figure are for $a_0 = 0.002\mu m, 0.0035\mu m$ and $0.005\mu m$ with fixed value of $a_m = 0.25\mu m$. It can be seen that the agreement between exact results and predictions of formulas is excellent. Although not shown here, it has been noted that while the variation in a_0 results in bigger changes in extinction, the variation in extinction due to variation in a_m is comparatively much weaker.

For silicate grains, the comparison of predictions from (16), (17) and (18) have been compared with exact results of computations from (4) in figure 2. In this figure, the three admitted values of a_0 are $0.004\mu m$, $0.005\mu m$ and $0.006\mu m$ with fixed $a_m = 0.30\mu m$. Predictions of formula can be seen to be extremely good. Here also the variation in extinction with a_m is much weaker in comparison to that with a_0.

To give an idea of errors in predictions of the formulas obtained, we have displayed percent error details in figures 3, 4 and 5 respectively for graphite perpendicular, graphite

parallel and silicate grain formulae. The percent error has been defined as:

$$Percent\ error = \frac{[K_{ext}(exact) - K_{ext}(formula)] \times 100}{K_{ext}(exact)}$$

In general, the error is within 1% but for a few regions it can go upto about 3%. The results are representative results for particular values of a_0 and a_m. However, It has been varified that this result is valid for entire range of a_0 and a_m values considered in this work.

5 Conclusions and discussions

In this work, we have presented the extinction spectrum analysis for astronomical silicate and graphite grains in the wavelength range $\sim$ 1000 - 4000 Å which covers the FUV and UV regions. The grain size distribution range covered by us is in keeping with the acceptable compositional aspects of interstellar dust models corresponding to average interstellar spectra data. From this point of view, we feel that the results and the analytic formulae presented in this paper have application-worthiness in the sense that accurate estimates of extinction contributions for these material components in the FUV and UV regions can directly be made. Needless to say that a fuller and more complete account of the extinction contributions made by each and every material components in respect of the various dust models are needed for ascertaining their effectiveness in reproducing the average interstellar dust extinction spectrum. This necessitates further large -scale investigative work-outs and mathematical analyzes of similar nature as provided by us in this work.

However, as is mentioned in section 1, our prime motivation behind this work has been to analyze the extinction spectrum for a size distribution of spherical particles having variable refractive index ($m = m(\lambda)$). Earlier, the same problem with constant m (at all wavelengths) was analyzed to have simple extinction-frequency relationships in different frequency ranges involving the first few lower order moments as well as some coefficients which seemed to be arbitrarily dependent on the refractive index. In case of power-law distribution $f(a) = a^{-3.5}$

all the moments ($\bar{a}$, $\bar{a^2}$, $\bar{a^3}$, $\bar{a^4}$) become simple functions of the end points a_0, a_m. Consequently, we have looked for functional forms of extinction in terms of variables a_0, a_m and $\nu(1/\lambda)$ in various sub-regions as has been given in section 3. This analysis can also be extended to more complex distributions that have been used by some authors [5,6]. In the present work, we have restricted ourselves to UV and FUV regions and power-law distribution for substantive demonstration of workability of the formulae developed along the line of our earlier work. It is our wish to extend this further to cover the visible and infrared regions of extinction spectrum for both these grain components as well in near future.

References

[1] Roy AK and Sharma SK, A simple analysis of extinction spectrum of a size distribution of Mie particles. J Opt A: Pure and Appl Opt 2005; 7: 675-684.

[2] Mathis JS, Rumpl W and Nordsieck KH, The size distribution of interstellar grains. ApJ 1977; 217: 425-433.

[3] Draine BT and Malhotra S, On graphite and the 2175 Å extinction profile. ApJ 1993; 414: 632-645.

[4] Draine BT at http://www.astro.princeton.edu/draine.

[5] Mathis JS, Dust models with tight abundance constraints. ApJ 1996; 472: 643-655.

[6] Weingartner JC and Draine BT. Dust grain-size distributions and extinction in the milky way, large magellanic cloud and small magellanic cloud. ApJ 2001; 548: 296-309.

Figure captions

Figure 1. Comparison of predictions of equations (8)- (11) and (12)-(15) in "$\frac{2}{3} - \frac{1}{3}$" approximation with exact computations from (4). Solid lines are predictions and points are exact computations. In this figure, $a_m = 0.25\mu m$ and $a_0 = 0.005\mu m$ (solid line), $a_0 = 0.0035\mu m$ (large dashed line) and $a_0 = 0.002\mu m$ (small dashed line).

Figure 2. Comparison of predictions of equations (16), (17) and (18) with exact computations from (4). Solid lines are predictions and points are exact computations. In this figure, $a_m = 0.30\mu m$ and $a_0 = 0.006\mu m$ (solid line), $a_0 = 0.005\mu m$ (large dashed line) and $a_0 = 0.004\mu m$ (small dashed line).

Figure 3. Percent errors in equations (8), (9), (10) and (11) with respect to exact computations from (4). In this figure, $a_m = 0.25\mu m$ and $a_0 = 0.005\mu m$.

Figure 4. Percent errors in equations (12), (13), (14) and (15) with respect to exact computations from (4). In this figure, $a_m = 0.25\mu m$ and $a_0 = 0.005\mu m$.

Figure 5. Percent errors in equations (16), (17) and (18) with respect to exact computations from (4). In this figure, $a_m = 0.30\mu m$ and $a_0 = 0.005\mu m$.

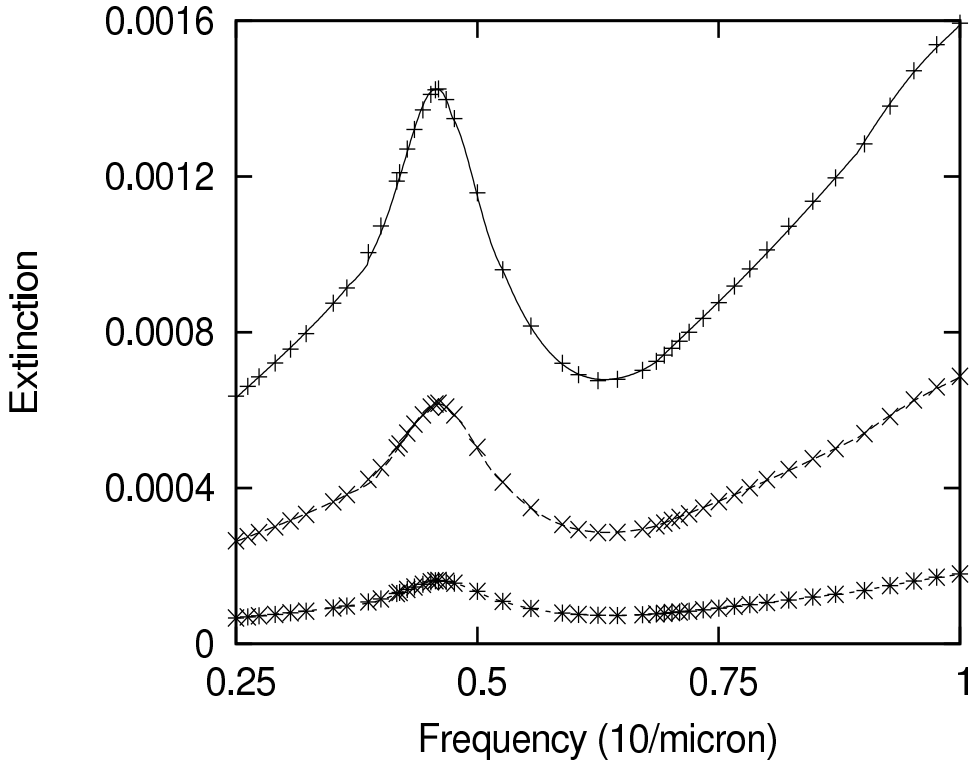
0.0016
0.0012
0.0008
0.0004
0
Extinction
0.25
0.5
0.75
1
Frequency (10/micron)

Figure 1:

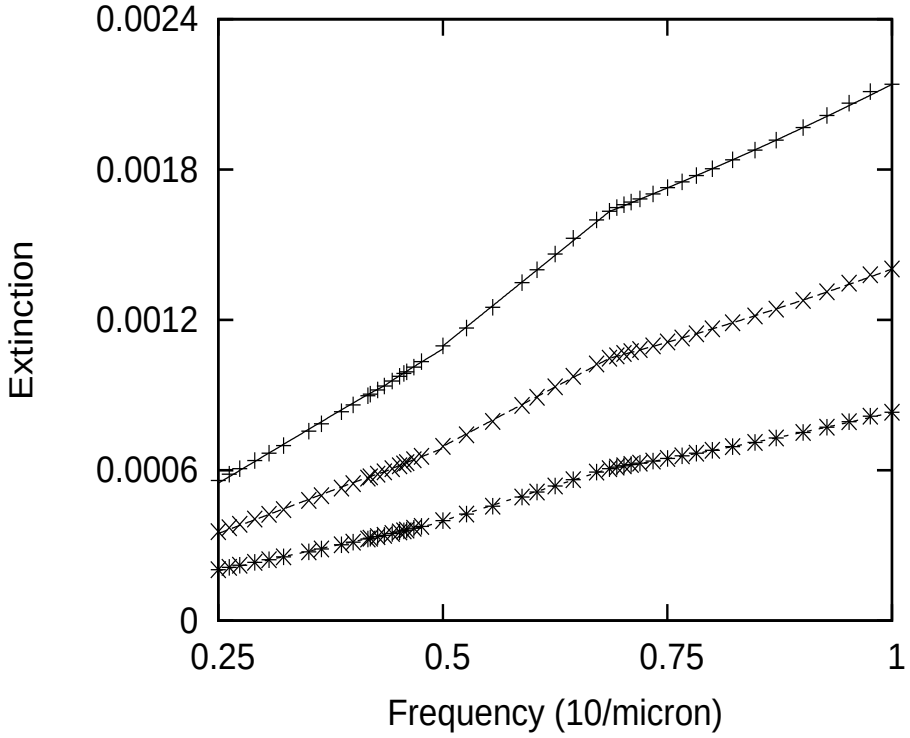
0.0024
0.0018
0.0012
0.0006
0
Extinction
0.25
0.5
0.75
1
Frequency (10/micron)

Figure 2:

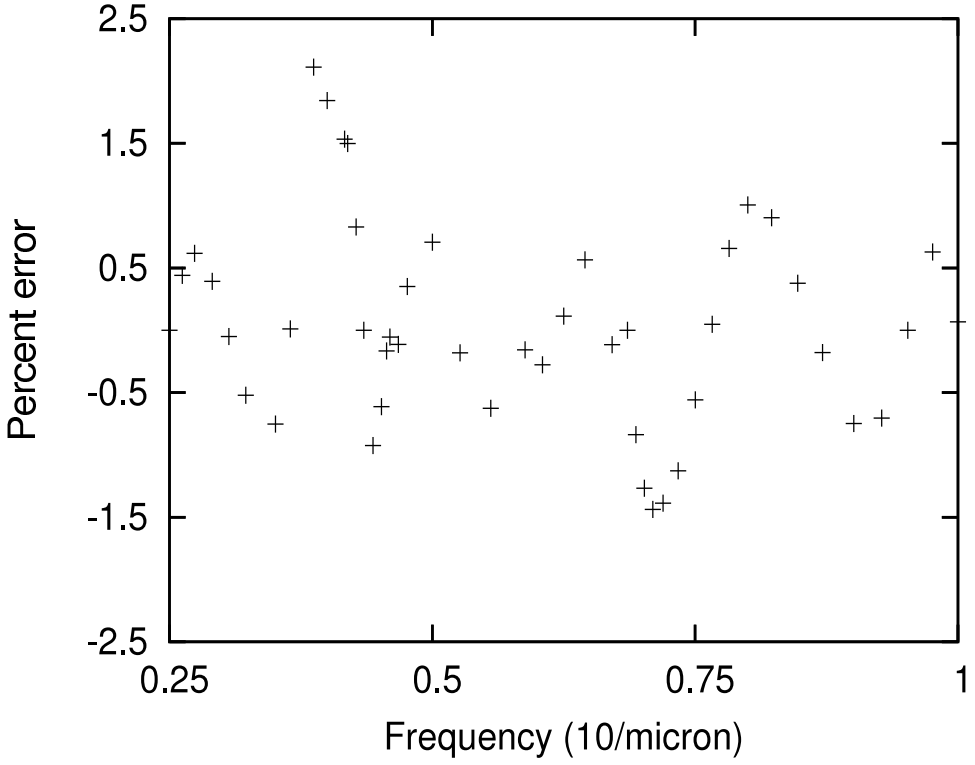
2.5
1.5
0.5
-0.5
-1.5
-2.5
Percent error
0.25
0.5
0.75
1
Frequency (10/micron)

Figure 3:

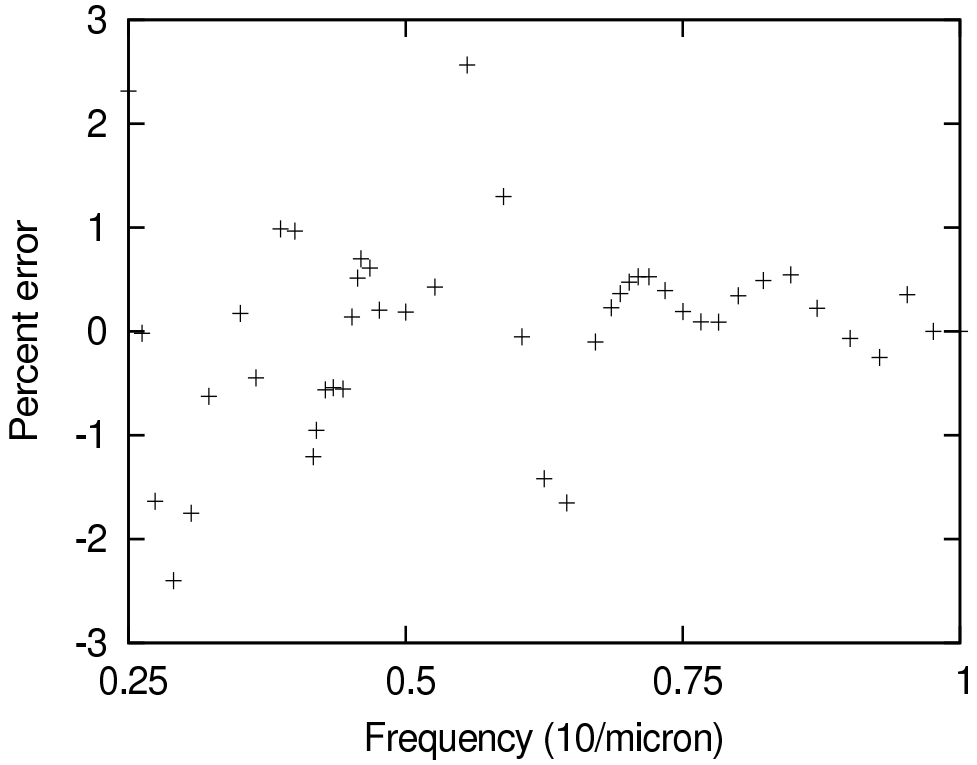

Figure 4:

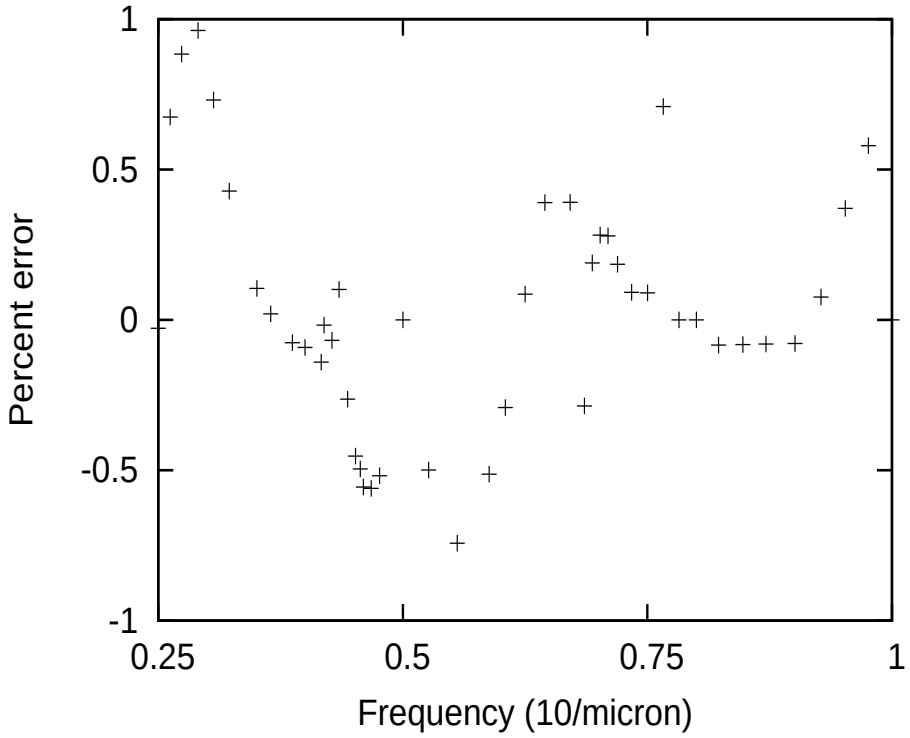

Figure 5: